scientific reports

Check for updates

OPEN

Crosstalk enables mutual activation of coupled quorum sensing pathways through "jump-start" and "push-start" mechanisms

Joseph George Sanders, Hoda Akl, Stephen J. Hagen & BingKan Xue✉

Many quorum sensing microbes produce more than one chemical signal and detect them using interconnected pathways that crosstalk with each other. While there are many hypotheses for the advantages of sensing multiple signals, the prevalence and functional significance of crosstalk between pathways are much less understood. We explore the effect of intracellular signal crosstalk using a simple model that captures key features of typical quorum sensing pathways: multiple pathways in a hierarchical configuration, operating with positive feedback, with crosstalk at the receptor and promoter levels. We find that crosstalk enables activation or inhibition of one output by the non-cognate signal, broadens the dynamic range of the outputs, and allows one pathway to modulate the feedback circuit of the other. Our findings show how crosstalk between quorum sensing pathways can be viewed not as a detriment to the processing of information, but as a mechanism that enhances the functional range of the full regulatory system. When positive feedback systems are coupled through crosstalk, several new modes of activation or deactivation become possible.

Many bacteria regulate and synchronize population-wide behaviors by exchanging diffusible chemical signals with other individuals of the same or different species within the community[1]. By secreting these chemical signals, known as autoinducers, and detecting their local concentrations, the bacteria can induce phenotypes collectively, in response to environmental and population conditions. These quorum-sensing regulatory pathways are usually sensitive to a variety of environmental and cross-species cues in addition to their own autoinducers, so that they control multiple phenotypic outputs in a complex fashion[2].

Quorum sensing bacteria typically synthesize and detect more than one chemically distinct autoinducer, often with positive feedback controlling the rate of autoinducer production. The different autoinducers are detected by cognate receptors that drive regulatory pathways coupled to varying degrees[3]. The ability to sense more than one autoinducer is hypothesized to provide a number of potential benefits to a microbial species. It may offer advantages in interspecies interactions, including greater resistance to manipulation by other species[4] or the ability for both interspecies and intraspecies communication[5]. Multiple signals may also allow temporal control of distinct phenotypes if different autoinducers accumulate at different rates[6,7], or they may help infer physical conditions such as spatial confinement[8], or provide advantages in quorum cheating[9]. Sensing through multiple signals and receptors in general may allow more sophisticated control of output dynamics of a sensing pathway[10]. But the ligand-specificity of quorum sensing receptors varies considerably among species and strains[4]; autoinducers employed by one organism often elicit a response from non-cognate receptor pathways in related variants or other microbial species. The lack of signal specificity allows interspecies "crosstalk" in bacterial communities[11], a phenomenon that has been widely explored in the context of social behaviors such as kin discrimination, eavesdropping and facultative cheating[3].

Crosstalk can also occur within a single species or strain. A pathway that senses one autoinducer may also be activated or inhibited by other autoinducers produced by the same organism. As these effects may occur through several different mechanisms, several definitions of crosstalk have arisen. In a system of two signal/receptor pairs that drive different promoters, and where specificity is poor, crosstalk has been characterized in terms of whether the lack of specificity resides in the ligand/receptor interactions or at the promoter-binding level[12]. It is also common, however, for pathways that detect multiple signals to funnel down to a fewer number of downstream outputs[10]. An extreme case is *Vibrio harveyi*, which senses three distinct autoinducers, each with its own dedicated sensor kinase; information from the three kinases is funneled into control of the same

Department of Physics, University of Florida, Gainesville, FL 32611, USA. ✉email: b.xue@ufl.edu

phosphorelay system[13]. Such funneled architecture has been described as crosstalk[14]. Here, we find it useful to define crosstalk as any mixing between two signaling pathways A and B that have their own signal inputs and outputs, but wherein signal A also modulates to some extent the output of receptor B, and vice versa. Crosstalk is a degree of coupling between two functional sensing pathways in the same organism[15–17], and the strength of crosstalk lies along on a continuum from very strong (funneled) to very weak (orthogonal pathways).

Because crosstalk mixes information received from separate signals, it would appear likely to degrade the performance of a quorum sensing pathway. It is however a highly evolvable property that can be reduced or even eliminated through (for example) receptor design[4,18,19]. Therefore, although there exist several hypotheses for why bacterial species use multiple autoinducer signals, there is still little understanding of why crosstalk is common in quorum sensing systems, and how it affects the output behaviors of these networks, beginning at the level of an individual organism.

Gram negative quorum sensing systems that employ autoinducers of the acyl homoserine lactone (HSL) type are particularly susceptible to crosstalk, as the HSLs are chemically similar and their cognate receptors typically respond to HSLs spanning a range of acyl chain lengths[11]. The quorum sensing system in the bacterium *Vibrio fischeri* is a model example[20] with homologs in numerous other species[4]. We will focus on two pathways in that organism, LuxI/R and AinS/R, which are subject to several forms of crosstalk, shown in Fig. 1. The *lux* operon that controls bioluminescence is under immediate control of the LuxI/R pathway, a feedback loop in which LuxI is the synthase for the autoinducer 3-oxo-C6-homoserine lactone (3OC6-HSL) that interacts with the intracellular receptor LuxR to bind the *lux* promoter. However, the production of LuxR is modulated by LitR, which is controlled by a second, upstream quorum sensing pathway, AinS/R. AinS and AinR synthesize and detect respectively an autoinducer N-octanoyl-L-homoserine lactone (C8-HSL) to control LitR production. The LuxI/R and AinS/R pathways crosstalk through several mechanisms. The LuxR-3OC6-HSL complex is able to modulate expression of AinS, which encodes the C8-HSL synthase, by interacting with a *lux*-box-type binding site[20,21]. In addition, C8-HSL can also interact with LuxR to promote its binding to the *lux*-box. Thus, C8-HSL exerts an influence on the downstream LuxR/LuxI system via LuxR and LitR, while 3OC6-HSL influences the production of the C8-HSL synthase upstream.

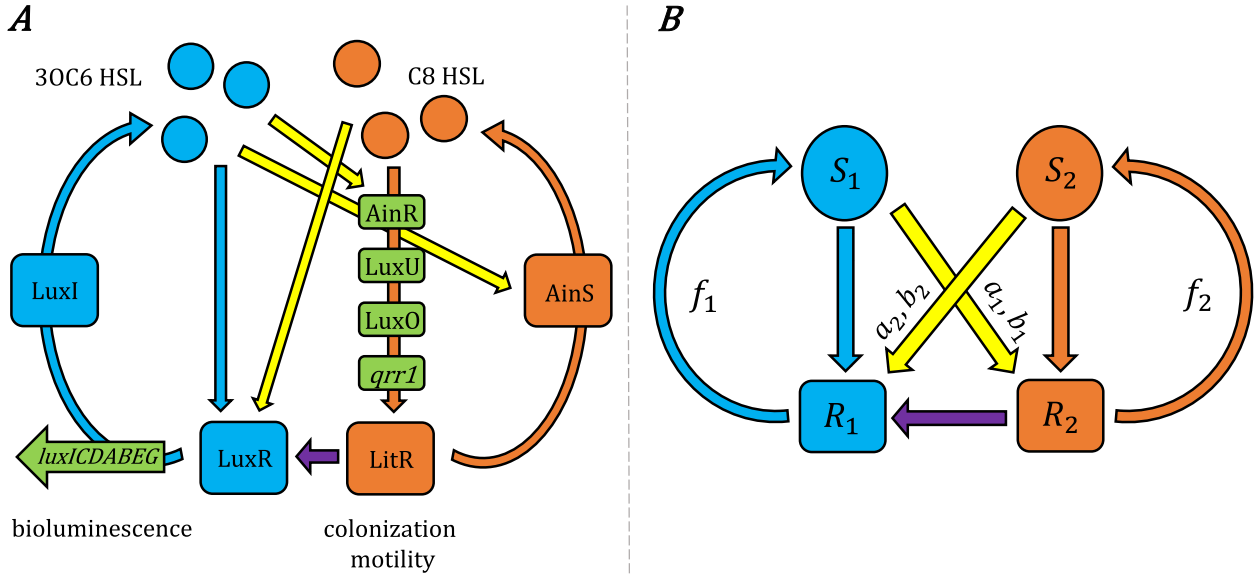

Figure 1. (**A**) The AinR/AinS and LuxR/LuxI quorum sensing pathways in *Vibrio fischeri*, which primarily control colonization traits and bioluminescence respectively, interact through several crosstalk mechanisms[20,22]. (A third pathway involving LuxS, LuxP/LuxQ and the autoinducer AI-2, coupled to the above through LuxU/LuxO, is not shown here.) The histidine kinase AinR detects its cognate autoinducer C8-HSL produced by AinS, initiating the LuxU/LuxO phosphorylation pathway. This pathway controls the expression of the regulatory RNA *qrr1*, a post-translational repressor of *litR*. In addition to controlling phenotypes related to motility and host colonization, LitR modulates production of LuxR, which is the intracellular receptor for the autoinducer 3OC6-HSL of the LuxI/LuxR pathway. LuxR becomes a transcriptional activator for the *lux* operon when bound either to its cognate signal 3OC6-HSL, produced by LuxI, or to the non-cognate C8-HSL. In addition, 3OC6-HSL interacts with LuxR to modulate activation of *ainRS*. Thus the AinR/AinS and LuxR/LuxI pathways both respond to each others' autoinducers, while the AinR/AinS pathway also acts upstream of the LuxR/LuxI pathway through LitR. (**B**) The simplified model studied in this work captures the key elements of a quorum sensing system with crosstalk: Two signals (S_1, S_2) elicit their respective cognate responses (R_1, R_2), with crosstalk between them (yellow arrows) and an additional link between R_1 and R_2 that makes R_2 upstream of R_1. The signals are produced with positive feedback (f_1, f_2) from their respective responses. The crosstalk parameters b_i and a_i respectively define the strength of cross-binding (between each signal S_i and its non-cognate receptor) and cross-activation (of the non-cognate response); see "Methods".

In order to understand how the tuning of crosstalk strength affects a two-pathway quorum sensing system, we have analyzed a simplified model of the *V. fischeri* system. The model retains key features of two signals that primarily stimulate two responses, with crosstalk as well as positive feedback in autoinducer synthesis. We use this streamlined model to explore how different aspects of the crosstalk interact with feedback to reshape the steady state outputs that are available to the system.

Model

We consider a model represented by the schematic in Fig. 1B, capturing the essential elements of crosstalk in the AinR/AinS and LuxR/LuxI quorum sensing pathways of *V. fischeri*. There are two signaling pathways, each of which produces a signal (S_1 or S_2) that induces a response (R_1 or R_2, respectively). The signal associated with each pathway is produced with positive feedback (f_1, f_2) from the response. One pathway (R_2, S_2) is functionally "upstream" of the other (R_1, S_1), in that response R_1 is dependent on R_2 (we do not call this link "crosstalk" because R_1 cannot function without it, so this link is not a tunable perturbation, see "Discussion" on "the meaning of crosstalk"). In addition, each of the two signals has some effect on the response of the other ("non-cognate") pathway.

The elements of multiple signals, feedback and crosstalk are captured by the equations:

$$S_1 = f_1 R_1 \tag{1a}$$

$$S_2 = f_2 R_2 \tag{1b}$$

$$R_1 = g_1 \frac{k_1 S_1^n + a_2 b_2 S_2^n}{1 + k_1 S_1^n + b_2 S_2^n} R_2 \tag{1c}$$

$$R_2 = g_2 \frac{a_1 b_1 S_1^m + k_2 S_2^m}{1 + b_1 S_1^m + k_2 S_2^m} \tag{1d}$$

These equations represent idealized steady states of a two-pathway sensing system (see detailed explanation in "Methods"). Although a real system in nature may never reach a steady state due to constant changes in environmental conditions over space and time, the steady states of a simplified model can help us understand generally how crosstalk shapes the system's behavior. In these equations, S_1 and S_2 represent the concentrations of the two autoinducers; R_1 and R_2 represent the expression levels of the quorum-regulated genes of each pathway, including genes that encode the autoinducer synthases. Equations (1a, 1b) relate the signal concentrations to the regulated genes, due to positive feedback. Equations (1c, 1d) give the steady state response to the two signal levels. Among the parameters, f_i is the feedback strength for each autoinducer, which depends on the rate of signal synthesis and the population density of cells; g_i is the maximum expression level of R_i; k_i is the interaction strength of a receptor with its cognate signal. For noncognate (crosstalk) interactions, the strength of binding and activation are described separately: b_i ("binding") captures the ability of a signal to competitively bind its non-cognate receptor; a_i ("activation") describes the efficiency of a signal, when bound to the non-cognate receptor, in cross-activating the non-cognate response. Finally, the exponents n and m represent the cooperativity of the signal response in each pathway.

We can simplify the equations by rescaling S_1 and S_2 to set $k_1 = k_2 = 1$, and rescaling R_1 and R_2 to set $g_1 = g_2 = 1$ (see "Methods"). Then the maximum value for the rescaled R_1 and R_2 is 1 (for $a_i \leq 1$). Of the remaining parameters, a_i and b_i control the crosstalk strength. If the binding $b_i = 0$, then the signal from pathway i cannot elicit any response from the non-cognate pathway, so there is no crosstalk. On the other hand, if the activation $a_i = 0$, the signal from pathway i may bind to but not activate the response of the non-cognate pathway. For $a_i > 0$ there is potential cross-activation between the pathways; we assume $a_i \leq 1$, which means the cross-activation by the non-cognate signal cannot be more efficient than the cognate signal. In most of what follows, we focus on the parameters a_2 and b_1, and set the other two parameters $a_1 = b_2 = 1$. That is, we focus on the case where S_2 interacts strongly with the noncognate receptor, but the complex is not necessarily an efficient activator for R_1. This is partly motivated by the example of *V. fischeri*, in which the effect of C8-HSL (analogous to S_2) on *lux* expression (analogous to R_1) is well known[23], and 3OC6-HSL (analogous to S_1) has been shown to stimulate the *ainRS* pathway (analogous to R_2)[21]. We will further assume that $m = n$, and consider a range of values for the cooperativity n.

The responses R_1 and R_2 are not simply functions of S_1 and S_2 as in Eqs. (1c,1d), except in the special circumstance where signal levels are externally controlled. In natural settings the signals are tied to the responses through the feedback f_1 and f_2. As a result, the equilibrium values of all signals and responses are determined by the feedback strengths by solving Eqs. (1a–1d). Eliminating S_1 and S_2 from Eqs. (1c,1d) using Eqs. (1a,1b) and simplifying the parameters as described above, we arrive at two self-consistent equations for R_1 and R_2:

$$R_1 = \frac{(f_1 R_1)^n + a_2 (f_2 R_2)^n}{1 + (f_1 R_1)^n + (f_2 R_2)^n} R_2 \tag{2a}$$

$$R_2 = \frac{b_1 (f_1 R_1)^n + (f_2 R_2)^n}{1 + b_1 (f_1 R_1)^n + (f_2 R_2)^n} \tag{2b}$$

We find the solutions to these equations using numerical solvers from the SciPy package for Python. We first solve a set of ODEs for which Eq. (2) are the equilibrium (see "Methods"). We integrate these ODEs for a sufficient amount of time that the variables come close to an equilibrium. Then, we use these values as initial guesses for a root solver to find the precise solutions. This method allows us to find multiple solutions if they exist and are stable, by using many random initial values in solving the ODEs. Once the solutions are refined using the root solver, we remove redundant solutions that have already been found (see "Methods" for details).

Results

The solutions to our main Eqs. (2a, 2b) represent the responses R_1 and R_2 as functions of the feedback strengths f_1 and f_2. Increased feedback strength may correspond to the condition of high cell density, where the autoinducer is captured by neighboring cells rather than being lost to the environment. When the cell density reaches a certain level, a phenotypic response is triggered. Our goal is to see how this response is modulated by the crosstalk parameters a_2 and b_1. Without crosstalk, the pathways operate independently: response R_i will be activated if the feedback f_i reaches a certain level. Crosstalk allows the feedback f_1 not only to elicit the cognate response R_1 but also to influence the other response R_2, and vice versa. We will characterize such effects below.

Crosstalk can both activate and inhibit non-cognate responses

Figure 2 shows a heat map of R_1 as a function of f_1 and f_2. R_1 is of interest as it is the most downstream element in our circuit (Fig. 1B), affected by both signals and the upstream response R_2. When both crosstalk parameters are at full strength, $a_2 = b_1 = 1$ (given that we also assume $a_1 = b_2 = 1$), R_1 is determined simply as a linear combination of f_1 and f_2 (Fig. 2 bottom-right panel). It means that R_1 is equally well activated by either one of the quorum signals, either directly by the cognate S_1 or through crosstalk by the non-cognate S_2. This strong crosstalk is analogous to what occurs in *V. harveyi* quorum sensing network, where three autoinducer inputs add linearly to give a single output[24].

Figure 2 also shows how the strength of the crosstalk a_2 determines whether the non-cognate signal S_2 activates or inhibits the response R_1. Strong activating crosstalk a_2 (Fig. 2 bottom row) allows R_1 to increase with f_2. Weakly activating crosstalk, where a_2 is small (Fig. 2 top row), allows a large f_2 to inhibit R_1. This is because at the low a_2 limit cross-activation is inefficient, so that non-cognate binding ($b_2 = 1$) allows competitive inhibition of R_1 by S_2.

Another feature to note is that, when the crosstalk binding strength b_1 is very small (Fig. 2 left column) and f_2 is also small, no amount of f_1 can activate R_1. This is because R_1 relies on the upstream response R_2, which remains off under conditions of small f_2 and b_1. However, as b_1 increases (right column), part of the small-f_2 region can now be activated by f_1 alone: Crosstalk from the downstream signal S_1 to the upstream response R_2 can activate the downstream response R_1. In "Discussion" on "new motifs" we elaborate on this mechanism where crosstalk from the downstream signal activates both responses.

Crosstalk can modulate the dynamic range of joint responses

To study the dynamic range of both responses R_1 and R_2 together, we make a parametric plot of their values as the feedback f_1 and f_2 are varied (Fig. 3). This creates a mesh of possible solutions that deforms as the crosstalk strengths a_2 and b_1 change. The mesh lies in the upper left half of each panel, because $R_1 \leq R_2$ as a result of Eq. (2a): the downstream response R_1 relies on the upstream R_2. R_1 and R_2 show greatest range and span a broader, two-dimensional region of the graph when crosstalk is weak, i.e., with a_2 small (Fig. 3 top row). As the crosstalk strength increases, the R_1, R_2 responses become more tightly coupled and span a reduced area. The effect is most apparent when both a_2 and b_1 approach 1 (Fig. 3 bottom right), for which the 2D mesh collapses toward a single curve. R_1 and R_2 are then tied together, and are both linear in f_1 and f_2 as seen from Fig. 2 (bottom right; see also Fig. S1).

Crosstalk can facilitate new mechanisms of activating responses

To visualize how both responses R_1 and R_2 depend on the feedback f_1 and f_2, we create "ellipse plots" in Fig. 4, in which an array of ellipses displays the values of both R_1 and R_2 at different positions in the (f_1, f_2) plane. For each ellipse, the horizontal axis is proportional to the value of R_1, and the vertical axis is proportional to R_2. Thus, the width of each ellipse in each panel of Fig. 4, as a function of f_1 and f_2, matches the R_1 value shown in the heat map of Fig. 2, while the height of each ellipse represents R_2 (Fig. S1). Where there are multiple stable solutions at the same (f_1, f_2) point, we overlay multiple ellipses on top of one another. In particular, a small black dot (a vanishing ellipse) indicates that the trivial solution $R_1 = R_2 = 0$ is stable.

The ellipse plots of Fig. 4 contain all the information in our results. As with the heat map in Fig. 2 and the mesh plots in Fig. 3, we see that when a_2 increases (from top to bottom rows), the upper left part of each graph shows a stronger R_1 response. In addition, from the ellipse plots in Fig. 4 it is clear that when the upstream crosstalk b_1 increases, the lower right part of each graph with a small feedback f_2 changes from having no response to having both R_1 and R_2 activated.

Figure 5 presents a different slice through the parameter space by showing R_1 and R_2 as functions of a_2 and b_1 in each panel, for selected values of f_1 and f_2 which vary between the panels. (The f_1 and f_2 values used for these plots are indicated by green squares in Fig. 4.) Thus, each panel allows us to move across the different panels in Fig. 4, showing how the crosstalk strengths change the responses at fixed feedback strengths. For a large f_2 and relatively small f_1 (Fig. 5 top left), the R_1 response can be activated by increasing a_2 even though R_1's cognate feedback f_1 is weak. Similarly, in the case of high f_1 and low f_2 (Fig. 5 bottom right), increasing b_1 will activate not only the response R_1 as expected from a high f_1, but also the response R_2 despite weak f_2.

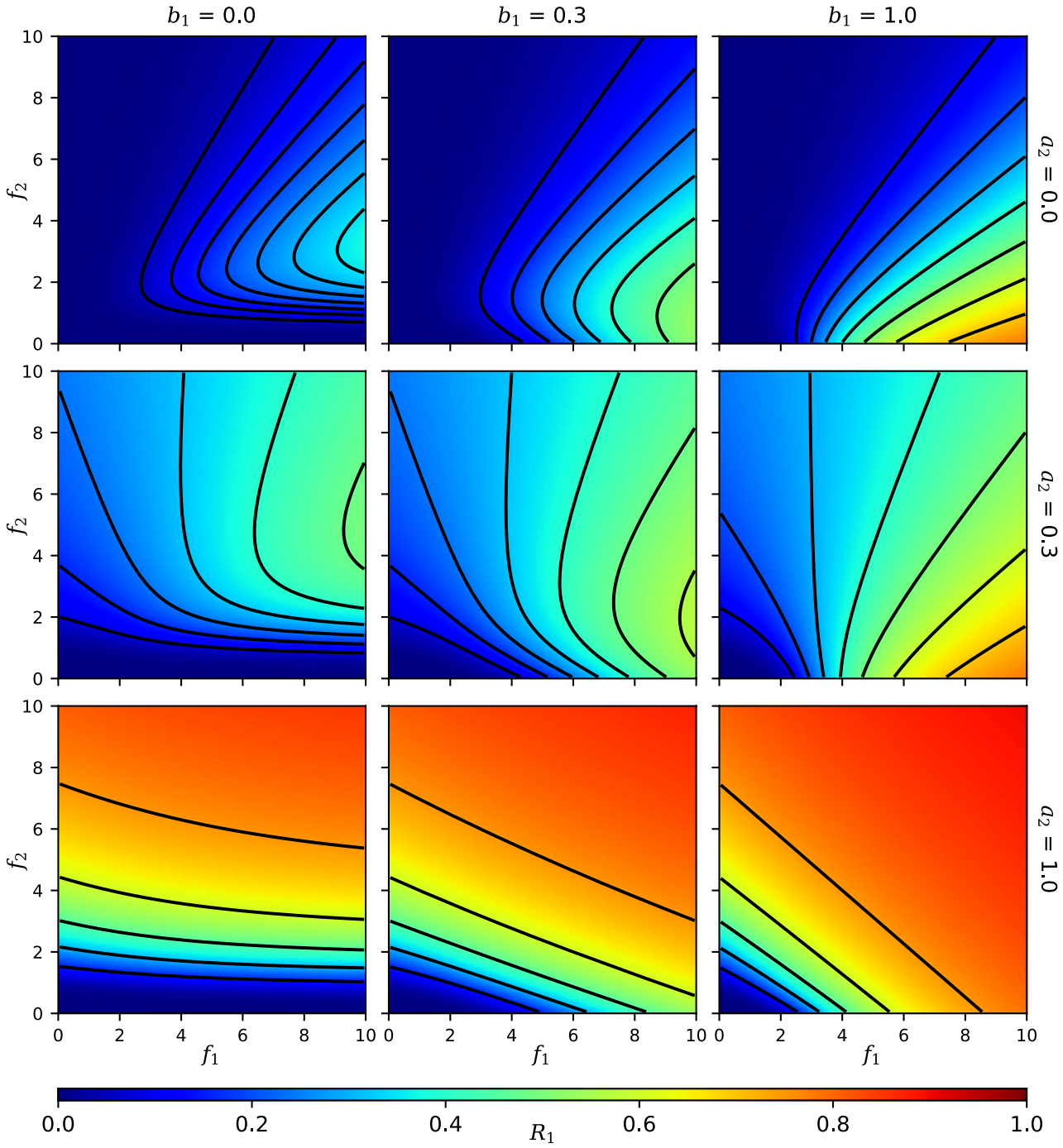

Figure 2. Heat maps showing the value of R_1 as a function of the feedback strengths f_1 and f_2. Rows correspond to different values of the downstream-directed crosstalk activation strength a_2, whereas columns correspond to values of the upstream-directed crosstalk binding strength b_1 (all panels have $a_1 = b_2 = 1, n = 1$). Black lines are contours of constant R_1.

Discontinuity and multistability at high cooperativity

Crosstalk can not only couple the two responses, as described above, but also restrict the joint responses to just a few distinct states. This can be observed for higher levels of cooperativity n. As examples, we show the results for $n = 2$ (Fig. 6 top row), which matches some experimental estimates[25], and for $n = 5$ (Fig. 6 bottom row), which represents a high cooperativity limit. The mesh of Fig. 3 breaks up into multiple tight clusters (Fig. 6 left column). As a result, there are only three distinct stable states that exist: The on state is characterized by activation of both R_1 and R_2; the half-on state has R_2 activated and R_1 partially activated; the off state has no activation of either R_1 or R_2. Due to the asymmetric, hierarchical positioning of the pathways, there is no fourth state where R_1 is active while R_2 is inactive.

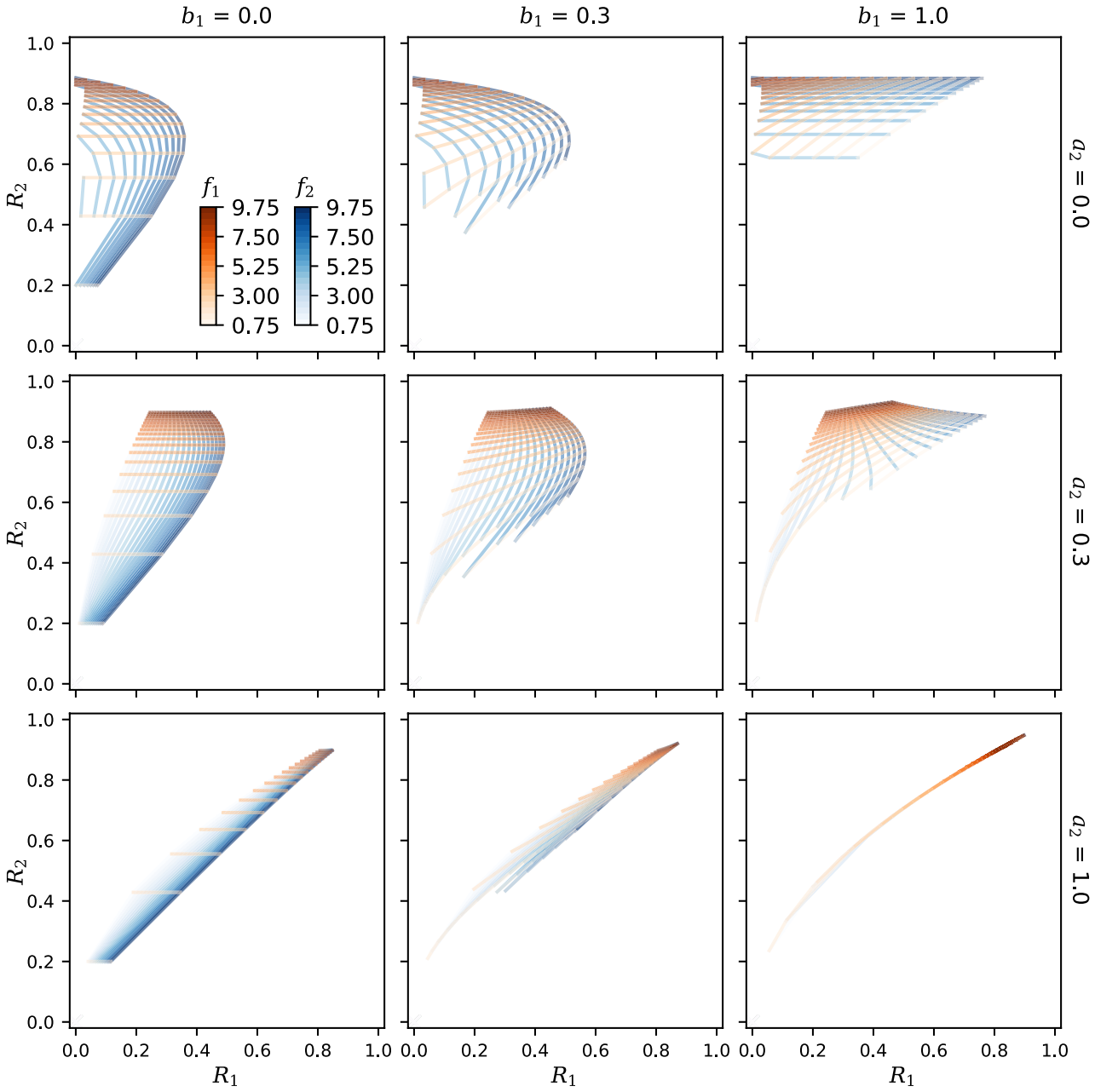

Figure 3. Mesh plots showing the steady state R_1 and R_2 at different feedback strengths. Orange curves represent constant f_1 values, and blue curves represent constant f_2 values. Rows and columns correspond to different values of the crosstalk parameters a_2 and b_1, respectively (with $a_1 = b_2 = 1, n = 1$).

As can be seen from Fig. 6 (middle column), at high cooperativity the responses R_1 and R_2 no longer change smoothly with the feedback strengths f_1 and f_2, but switch discontinuously along certain boundaries in the (f_1, f_2) parameter space (see also Fig. S2 for $n = 5$). In the limit $n \to \infty$, the phase diagram of Fig. 7 is obtained (see "Methods"), where each region of the parameter space permits different types of solutions to Eq. (2). In Region I, both feedbacks f_1 and f_2 are too small to activate a response, allowing only the trivial solution with R_1, R_2 both off. In Region II, with high f_2 and relatively low f_1, there exists an additional half-on state, with the upstream R_2 fully activated and the downstream R_1 only partially active. In Region IV, f_1 and f_2 are both sufficiently large to allow simultaneous activation of both responses R_1 and R_2, i.e., a fully on state instead of half-on. Between regions II and IV is region III, which allows both the half-on state and the fully on state, in addition to the off state.

Importantly, changes in the crosstalk strengths cause the boundaries in the phase diagram to move, because crosstalk allows the upstream and downstream feedback loops to activate each other. The sloped boundary between Region III and IV depends on the crosstalk parameter a_2: as a_2 increases, this boundary rotates counterclockwise around the origin, expanding Region IV and reducing Region III. In addition, the value of R_1 in Region II & III also increases with a_2. Similarly, the vertical boundary between Regions IV and I depends on b_1: if b_1 decreases to 0, this boundary moves all the way to the right, removing the small-f_2 portion of Region IV.

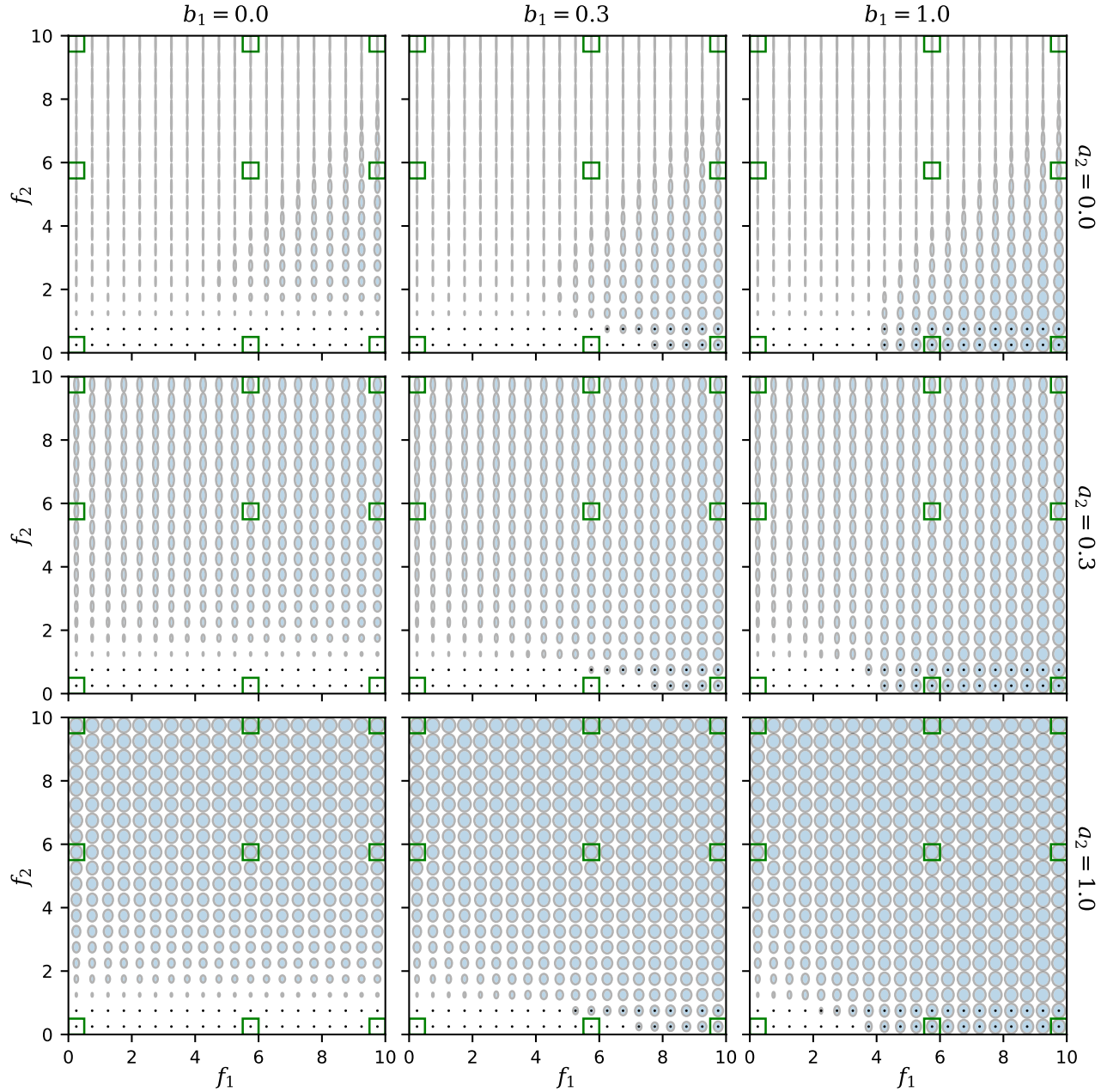

Figure 4. "Ellipse plots" showing the responses R_1 and R_2 simultaneously as functions of the feedback strengths f_1 and f_2. The width and height of each ellipse represent the values of R_1 and R_2, respectively, at a given point in the (f_1, f_2) plane. A black point superimposed on an ellipse indicates that the trivial state $R_1 = R_2 = 0$ is also stable. Rows and columns represent different values of the crosstalk parameters a_2 and b_1, respectively (with $a_1 = b_2 = 1, n = 1$). The f_1 and f_2 values marked in green are further explored in Fig. 5.

Discussion

The model studied here does not contain all the ingredients of any quorum sensing pathway and is not intended as a completely faithful representation of *V. fischeri* LuxRI and AinRS pathways. It does however capture several common properties of quorum sensing networks: (1) multiple signals and cognate receptors drive multiple regulated outputs; (2) these pathways are functionally linked (sequentially in *V. fischeri*); (3) the pathways crosstalk through the interaction of signals with non-cognate receptors; (4) both pathways are regulated with positive feedback. The model offers insight into how the strength of crosstalk interacts with these architectural properties to alter the behavior of a quorum sensing system.

The meaning of crosstalk

Quorum sensing pathways frequently employ multiple ligand-receptor pairs with limited binding specificity, where the "promiscuity" of this binding is a highly tunable or evolvable property[4,11,19]. Previous authors have investigated behavior of signaling pathways subject to this and other mechanisms of crosstalk; these include weak

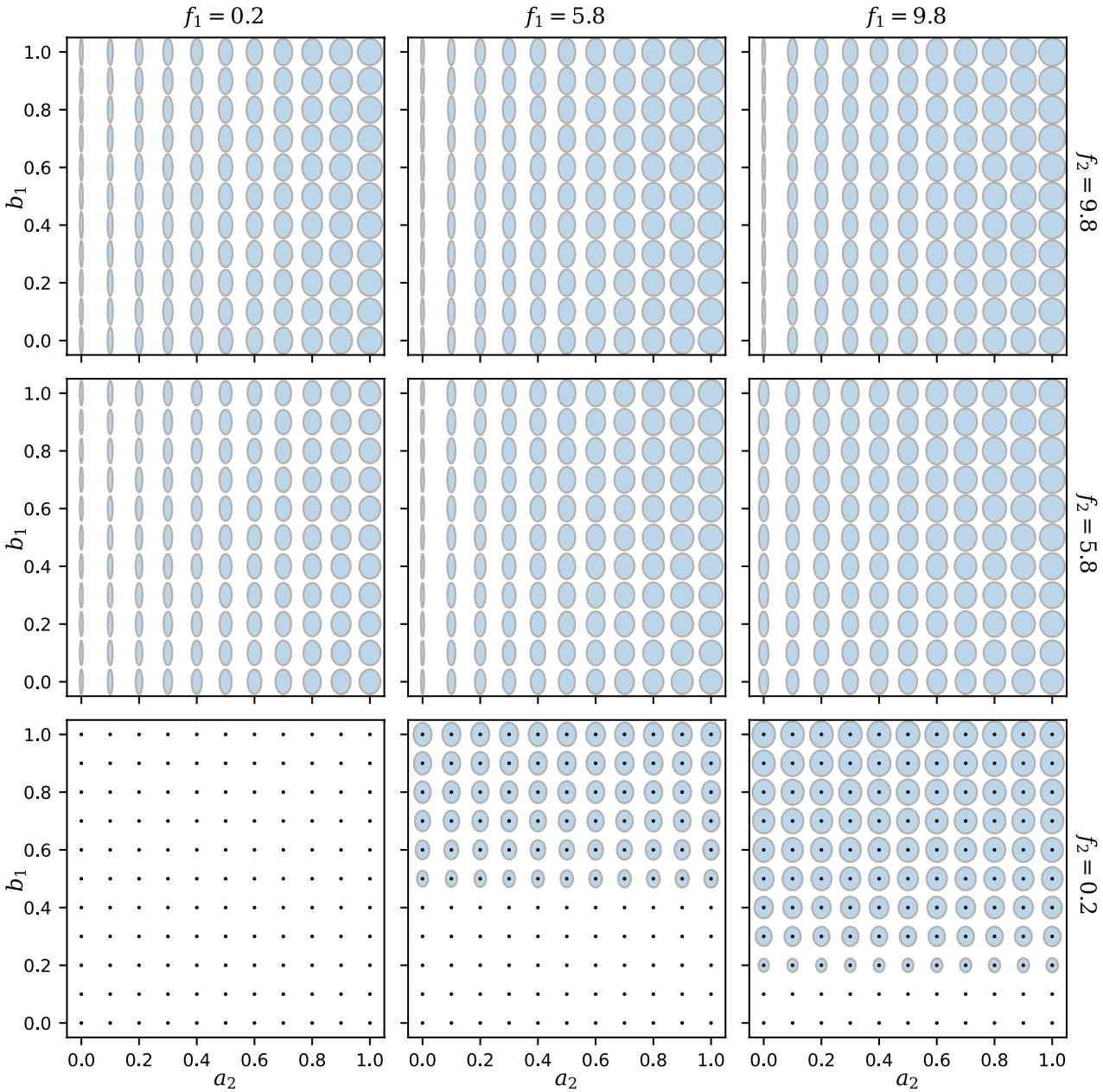

Figure 5. Dependence of the responses R_1 and R_2 on the crosstalk parameters a_2 and b_1. With the same parameters as in Fig. 4, the width and height of each ellipse represent the values of R_1 and R_2, respectively. Rows and columns here represent different combinations of the feedback f_1 and f_2 (marked green in Fig. 4). A black point superimposed on an ellipse indicates that the trivial state $R_1 = R_2 = 0$ is also stable.

selectivity in ligand affinities at a cell surface receptor[16], multiple ligand-receptor channels that merge to control a single regulated output[13,24], or a receptor that has multiple sensing states and outputs that are associated with binding of different ligands[14].

The ubiquity and tunability of crosstalk in quorum sensing systems raise the question of how even weak crosstalk may enhance the function of a multi-signal system. For example, a limited amount of crosstalk between two signaling pathways can in principle enhance the ability to measure the input signal concentrations[16]. It may also provide some benefit in suppressing early response[25]. Therefore, rather than consider a mechanistic model that embeds strong crosstalk into the topology, we study a model where distinct signaling pathways are coupled through tunable crosstalk parameters: crosstalk strength can range from a perturbation that weakly couples the two pathways to a strong link that drives two regulated outputs in tandem.

Crosstalk through cross-binding or cross-activation

Our analysis highlights the importance of distinguishing between two different aspects of crosstalk that occurs when a receptor interacts with its non-cognate ligand (signal): One is cross-affinity, or the lack of specificity in binding, of a signal by the non-cognate receptor (characterized by parameter b in Eq. 1c). The other is the ability

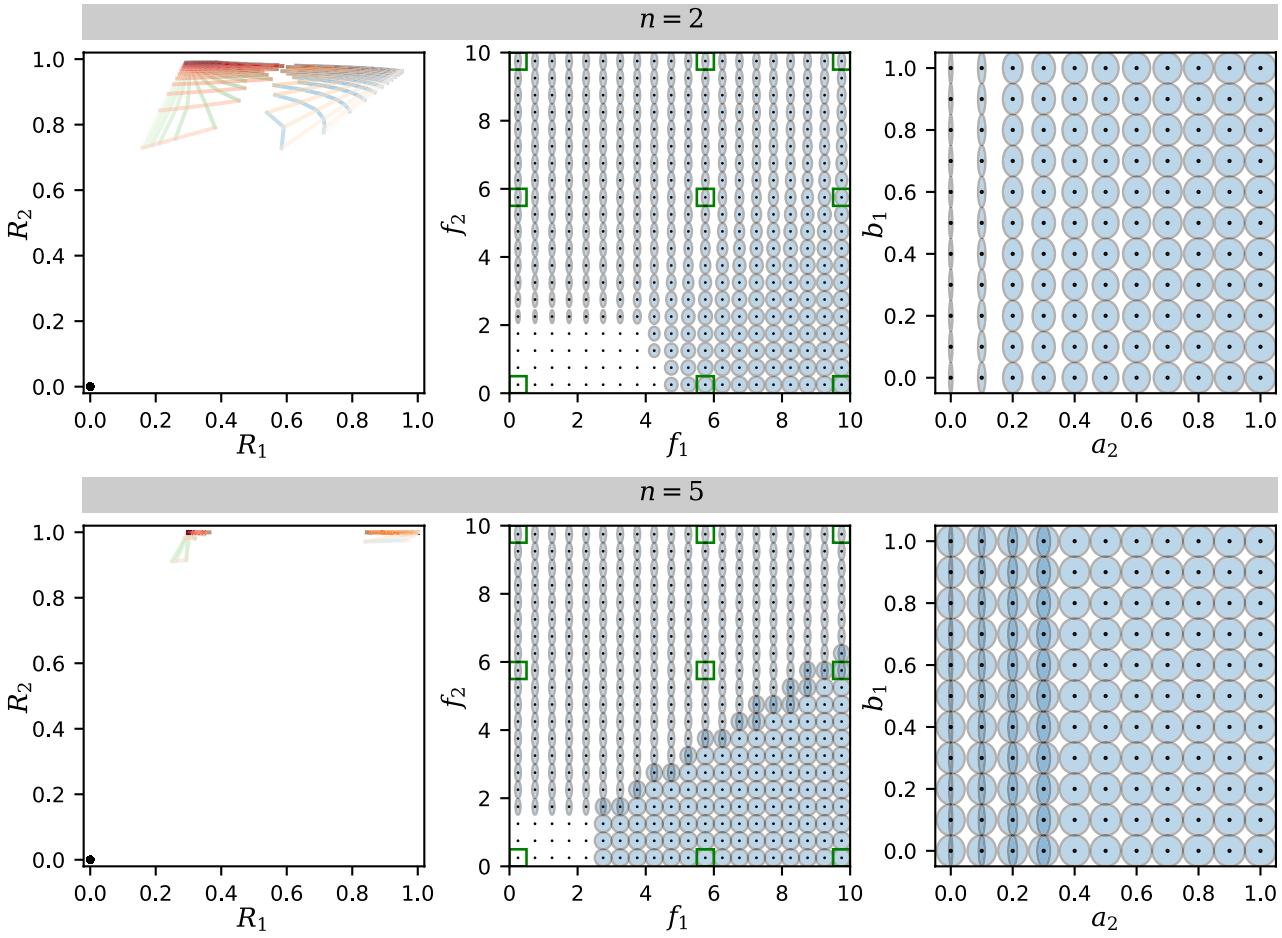

Figure 6. Examples of mesh and ellipse plots for higher cooperativity $n = 2$ and $n = 5$ (see Figs. S2 and S3 for detailed plots for $n = 5$). Left column: $a_2 = b_1 = 0.3$, to be compared with the center panel of Fig. 3 under the same color scheme. Middle column: $a_2 = b_1 = 0.3$, to be compared with the center panel of Fig. 4. Right column: $f_1 = 9.8$ and $f_2 = 5.8$, to be compared with the mid-right panel of Fig. 5. All panels have $a_1 = b_2 = 1$.

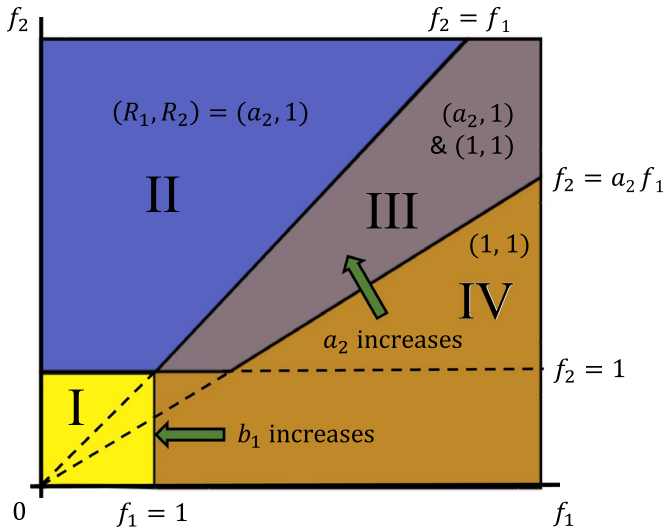

Figure 7. Phase diagram showing which states of (R_1, R_2) are permitted for different combinations of f_1 and f_2 values (in addition to the trivial solution $R_1 = R_2 = 0$), in the limit of high cooperativity $n \to \infty$. (I) there is only the trivial solution - R_1 and R_2 both off; (II) R_2 is on, R_1 is partially on (proportional to a_2); (III) R_2 is on, R_1 can be either fully or partially on; (IV) both R_1 and R_2 are fully on.

of the resulting non-cognate complex to cross-activate the regulated pathway (characterized by parameter a). If the receptor bound by the non-cognate signal is ineffective at promoting transcription, the result is competitive inhibition of the receptor. Mathematically, in Eq. (1c), the inhibition is due to S_2 appearing in the denominator of the expression for R_1. Thus, cross-binding allows the excitatory signal of one channel to inhibit the non-cognate response. On the other hand, if the receptor bound by a non-cognate signal can still promote transcription to some level, then there is cross-activation of the response, especially when the cognate signal is absent. Mathematically, when $S_1 = 0$, Eq. (1c) allows R_1 to be activated by signal S_2, although at a lower saturating level governed by a_2 (see "Methods"). Thus, the activation (a) and binding (b) components of crosstalk allow a response to be either activated or inhibited respectively by the non-cognate signal, when its own cognate signal is weak.

The dual effect of the non-cognate signal is observed in *V. fischeri*, where both C8-HSL and 3OC6-HSL are able to form an activating complex with LuxR. Because the C8-HSL-LuxR complex is less efficient at inducing *lux*, crosstalk from the *ainS/R* pathway inhibits the activating effect of 3OC6-HSL during the growth of a colony[26,27]. Although the C8-HSL autoinducer can stimulate luminescence at low concentrations of 3OC6-HSL[25], at high 3OC6-HSL concentrations, the addition of C8-HSL reduces luminescence through the competition effect[28].

Weak crosstalk expands dynamic range

The extreme case of *V. harveyi*, where two signals merge to drive a single regulated output, is an example of two dimensions of signal input leading to a one-dimensional regulatory output. In *V. fischeri* the strength of crosstalk is evidently tunable between strains, as the HSL specificity of the LuxR receptor is strain-dependent. Further, both the *lux* regulatory region and the AinS/AinR system exhibit much greater sequence divergence between strain isolates of *V. fischeri* than is typical of the rest of the genome[29]. These findings suggest that the quorum sensing pathways in *V. fischeri* are under strong, strain-dependent selection pressures with consequences for *lux* control and associated crosstalk.

What benefits can different strains gain by tuning weak crosstalk interactions between the two pathways? Figure 3 shows graphically how crosstalk strength modulates the space of system outputs. A sensing system with two fully independent outputs such as R_1 and R_2 has in principle a two-dimensional space of outputs. In the limit of strong crosstalk these two independent outputs are collapsed to fall along the same, one-dimensional arc. Thus, fine tuning of the strength of crosstalk between the signal paths can define the dimensionality, shape, and extent of the response region in Fig. 3, tuning the dual output response to f_1 and f_2 along a continuum from orthogonality to tandem or 'funneled' control. Funneled control may be beneficial when there is a risk that quorum interference is removing one signal from the environment, so that "OR" sensing is desirable; orthogonality will be advantageous when multiple phenotypic behaviors need to be controlled by the dual-signal system. Crosstalk allows some compromise between these two limiting behaviors.

Role of feedback

With both nonlinearity and feedback present in the model, one may expect to observe multistability, i.e., more than one steady state may be stable given the same parameter values. Especially in the limit of high cooperativity, we observe multistable states in several regions of the parameter space. Although multistability normally requires $n \geq 2$, in the presence of crosstalk there is multistability even for $n = 1$, such as when $b_1 > 0$ and f_1 is high but f_2 is low (Fig. 5 bottom right). This is because the coupling between the two feedback loops results in stronger nonlinearity than in a single feedback loop, allowing multistability (see "Methods").

Experiments however find few clear examples of multistability in quorum sensing, which would be indicated by a multimodal distribution of corresponding phenotypes. With some exceptions (usually based on synthetic or 'rewired' pathways[30–32]), multistability is rarely observed in Gram negative quorum systems. Generally the highly diffusible HSL signals, together with positive feedback synthesis, act intercellularly to lock the entire population into an on-state. Because of extracellular accumulation of autoinducer, the off-state becomes increasingly unfavorable or unlikely compared to the on-state. Multistability in quorum sensing circuits is more evident when the signal feedback at the individual cell level is strengthened, either by circuit redesign[31] or because the signal is able to act intracellularly, allowing isolated cells to autoactivate[33].

Another factor that makes it difficult to observe multistability in individual cells is that experiments often fix the extracellular signal concentrations at defined levels, or use strains in which feedback has been broken by deletion of the signal synthases. Thus, the difference between the multistability in experimental conditions and in our model highlights the important distinction between keeping the signals constant and letting them "float" according to the feedback. To observe multistability one must allow the signal levels to float either upward or downward, as natural systems do. However, in many laboratory experiments, the signal levels are externally controlled by supplying those molecules at known concentrations. As a result, multistability is suppressed and noise in gene expression is a much more significant source of heterogeneity[34,35].

New motifs: "jump-start" and "push-start"

Our results show that crosstalk can allow either of the feedback loops – upstream or downstream – to activate the other loop, via separate mechanisms driven by a_2 and b_1 respectively. As illustrated schematically in Fig. 8A, the first mechanism is engaged when the feedback strength f_1 is low but f_2 is high (Region II in Fig. 7). A large f_2 turns on the S_2-R_2 feedback loop, but without crosstalk the R_1 response is off due to a small f_1. Strengthening the downstream-directed crosstalk a_2 allows the upstream S_2-R_2 feedback loop to also activate the downstream R_1 response (Fig. 8A). This is roughly analogous to the "jump-start" of a combustion engine, where an upstream system consisting of a battery, alternator and starter motor is mechanically coupled to a downstream system consisting of the combustion engine and flywheel: activating the upstream branch by energizing the starter system turns the motor which then starts the combustion engine.

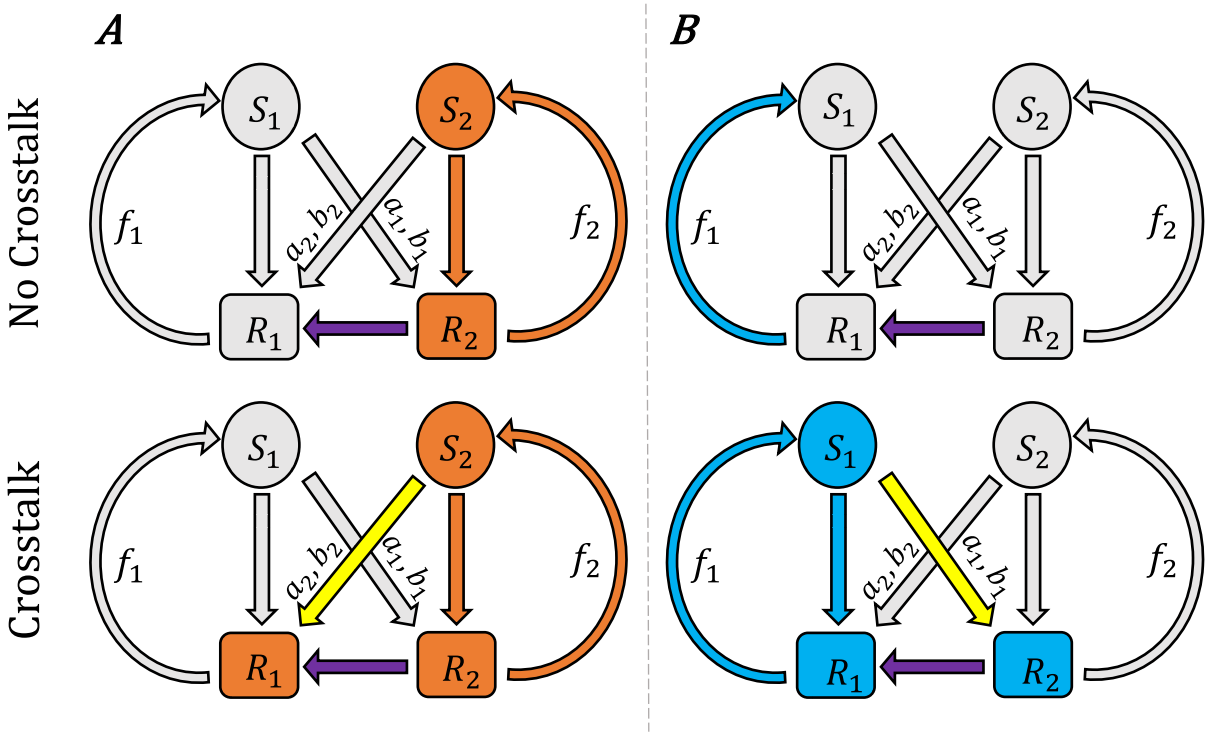

Figure 8. Crosstalk provides two new mechanisms for activating both pathways without requiring strong feedback in both. In the "jump start" scenario (left), even when the feedback f_1 is weak but f_2 is strong, the downstream-directed crosstalk (a_2, b_2) allows the S_2-R_2 pathway to activate and drive the downstream R_1 response. In the "push start" scenario (right), when the feedback f_2 is weak but f_1 is strong, the upstream-directed crosstalk (a_1, b_1) allows the R_2 response to be driven by the S_1-R_1 pathway, activating both R_1 and R_2.

The second mechanism, shown in Fig. 8B, applies when f_1 is large but f_2 is small (lower part of Region IV in Fig. 7). In the absence of crosstalk, even a large f_1 cannot turn on R_1, because it depends on the upstream response R_2 that is off due to a small f_2. However, sufficient upstream-directed crosstalk b_1 can allow the downstream R_1-S_1 feedback to drive the upstream R_2 and activate both R_1 and R_2 (Fig. 8B). This has a rough analogy in the "push-start" of a combustion engine with a dead starter battery: the mechanical coupling from the engine crankshaft to the upstream battery/alternator system allows an energy input at the wheels to turn the engine, which then turns the alternator, replacing the role of the battery and activating the downstream (engine) and upstream (alternator/battery) systems.

To illustrate these mechanisms, we simulate a dynamical system corresponding to our model (Eqs. (12–15) in "Methods"). The initial values are chosen to be the steady states for the system with small crosstalk, i.e., low a_2 for jump-start, and low b_1 for push-start. Then we switch on large values for these crosstalk parameters and run the dynamical system until it reaches a new steady state. Our simulation also includes random noise in the dynamics to show the stability of the steady states. For jump-start (Fig. 9 top row), the initial state is such that R_2 is already on but R_1 is off, due to a low f_1 and a small a_2. We then reset a_2 to a large value and the dynamics take the system to a new steady state where R_1 turns on. Note that S_1 remains low because R_1 is turned on by the crosstalk a_2, not by the feedback f_1. For push-start (Fig. 9 bottom row), both R_1 and R_2 are off in the initial state with a low f_2 and a small b_1. When b_1 is switched to a large value, the noisy dynamics allow the system to escape the off state and turn on both R_1 and R_2. In this case S_2 remains low because the responses are turned on by the crosstalk b_1 instead of the feedback f_2.

These two mechanisms can be thought of as new regulatory motifs that could be embedded within larger gene regulatory networks. The essence is that two feedback loops, linked by crosstalk, are positioned upstream and downstream from each other. Crosstalk between the feedback loops allows activation through the jump-start (upstream feedback loop activating downstream response) and push-start (downstream feedback loop activating both responses) behaviors. In addition to these motifs (where we set $a_1 = b_2 = 1$), there are other interesting behaviors when all the crosstalk parameters are considered, as summarized in Table 1. In particular, we have the opposite of the jump-start and push-start, which could be called "jump-stop" and "push-stop", where crosstalk from one branch can inhibit the function of the other branch.

Type	f_1	f_2	a_1	a_2	b_1	b_2	R_1	R_2
Jump Start	Low	High	1	↑	—	1	↑	1
Push Start	High	Low	1	—	↑	1	↑	↑
Jump Stop	High	High	—	0	—	↑	↓	1
Push Stop	High	High	0	—	↑	—	↓	↓

Table 1. Modes of activation and deactivation through crosstalk between two coupled quorum sensing pathways. The "jump start" and "push start" modes activate the system as illustrated in Fig. 8, whereas the "jump stop" and "push stop" modes shut down the system. The f_1, f_2 columns show the feedback conditions required for each mode, while the a_1-b_2 columns show how the crosstalk parameters must be configured, to generate the outputs shown in the R_1, R_2 columns. A dash means the parameter does not strongly impact the behavior.

Conclusion

Although crosstalk in engineering contexts refers to an undesired leakage of information between separate communication channels, in the context of biological sensing it can provide additional mechanisms for the control or activation of coupled feedback systems that are ubiquitous in quorum sensing pathways. In our analysis crosstalk appears to provide a route for switching individual feedback circuits on or off without relying entirely on extracellular signal concentrations as in typical interpretations of quorum sensing. Our findings are based on analyzing the equilibrium states of the feedback circuits that are coupled through crosstalk. How crosstalk affects the kinetics of the system as it approaches the equilibrium is likely an important component of its biological role, which remains to be studied.

The variability of crosstalk strength across different quorum sensing systems and even across strains of the same bacterial species suggests that the new mechanisms for activating the feedback circuits can be exploited through evolutionary tuning of the crosstalk strength. For example, crosstalk could provide a form of redundancy so that a pathway can still be activated when the signal is being inhibited, such as by quorum interference: If a sabotaging species removes the signal S_1 from the environment, or creates an interfering signal S_3 that saturates the S_1 receptor, the jump-start mechanism may ensure that the downstream response R_1 can still be activated. Likewise, the push-start mechanism may protect against external interference with the signal S_2 of the upstream response R_2.

It may also be possible that crosstalk strengths could be tuned on short timescales by cellular processes. For example, the cross-binding strength b could be affected by allosteric interactions with modifier proteins, while the cross-activation efficiency a could be controlled by other ligands or post-translational regulation. If crosstalk was variable in real time, instead of over evolutionary timescales, then it could be a very significant mechanism for control. It would be interesting if experiments could show that crosstalk strengths are variable within the same species and under different environmental conditions, allowing jump-start and push-start in real time. This could even lead to community-level phenomena, such as one species triggering the quorum sensing pathway of another by tuning their crosstalk strengths, i.e., an "interspecies jump-start".

Methods

Formulating the mathematical model

We consider a quorum sensing system in which two autoinducer signals drive the activity of two largely distinct, but coupled, regulatory pathways. In a simplified picture, where the two pathways operate without crosstalk, the autoinducer binds to a cognate receptor and the bound complex promotes the expression of a corresponding set of genes, including one that encodes the autoinducer itself. The specific mechanisms of signal transduction are variable, and may involve an intracellular receptor that binds the signal to form a transcriptional activator, or a membrane bound receptor that controls a phosphorylation cascade.

We think of the signals S_i as the concentrations of the two autoinducer species, and the responses R_i as the expression levels of the corresponding quorum regulated genes. We model the gene expression level as a function of the autoinducer concentration using a binding-equilibrium expression that resembles the Michaelis–Menten and Hill equations,

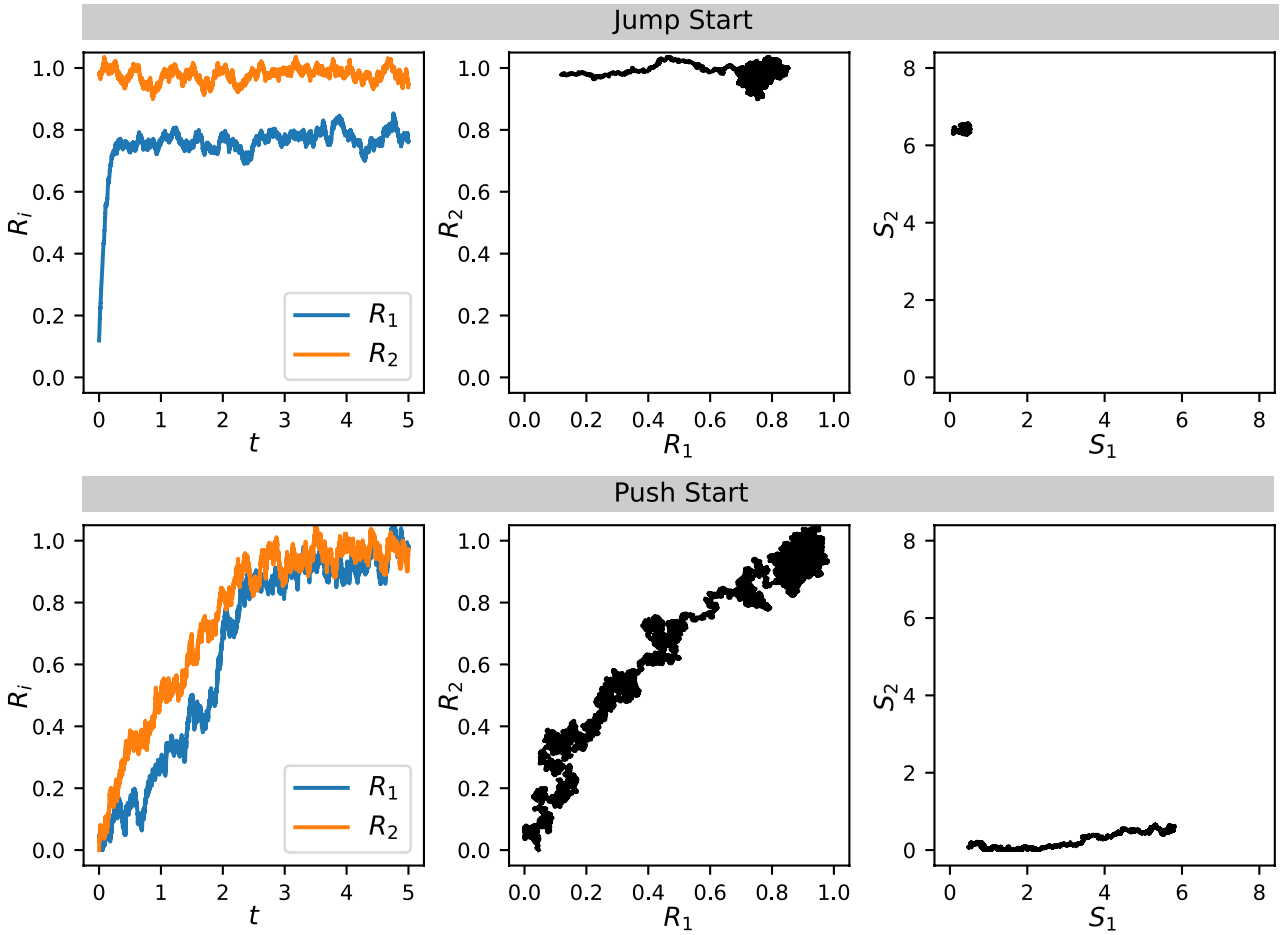

Figure 9. Simulation of the jump-start and push-start processes using a dynamical system with noise (see "Methods"). Top row: Jump-starting from an initial state with R_1 off by having a large crosstalk a_2. Parameters are $f_1 = 0.6, f_2 = 6.6, a_1 = 1, a_2 = 0.8$ (initially 0.1), $b_1 = 0.5, b_2 = 1, n = 2$. Bottom row: Push-starting from an initial state with R_1 and R_2 both off by having a large crosstalk b_1. Parameters are $f_1 = 6.6, f_2 = 0.6, a_1 = 1, a_2 = 0.5, b_1 = 0.8$ (initially 0.1), $b_2 = 1, n = 2$.

$$R_i = g_i \frac{k_i S_i^n}{1 + k_i S_i^n}, \tag{3}$$

where g_i is the maximum level at saturation and k_i represents the binding affinity of the autoinducer. For each pathway the expression level R_i of quorum sensing genes determines the production of the corresponding autoinducer S_i, through positive regulatory feedback. For simplicity, we assume that:

$$S_i = f_i R_i \tag{4}$$

where f_i is the strength of feedback and depends on the diffusion and degradation of the autoinducer molecules.

Crosstalk between the two quorum sensing pathways occurs when the autoinducer of one pathway can modulate gene expression in the other pathway. For example, a non-cognate autoinducer may bind to the receptor with some affinity, producing a resultant complex that promotes gene expression with some efficiency. Thus, the gene expression level will depend on the concentration of both autoinducers. We model such dependence by modifying Eq. (3) to:

$$R_i = g_i \frac{k_i S_i^n + a_j b_j S_j^n}{1 + k_i S_i^n + b_j S_j^n} \tag{5}$$

Here j is the label for the non-cognate signal – the $b_j S_j^n$ term in the denominator represents competitive binding by the non-cognate autoinducer, and the $a_j b_j S_j^n$ term in the numerator represents cross-activation by the non-cognate complex. The parameter b_j represents the binding affinity of the non-cognate autoinducer to the receptor, and a_j represents the promotion efficiency of the non-cognate complex. This form of dependence on multiple signals is fairly general as it can be derived for different, common quorum sensing system architectures[24,25]. Detailed derivation of these equations for the specific pathways in *V. fischeri* is described in the Supplementary Material.

We now incorporate some more details of the circuit that is present in the *Vibrio fischeri* example. In that system, pathway 2 is upstream of pathway 1 (Fig. 1A), so that the expression level of R_1 depends on that of R_2 (Fig. 1B). This is modeled by simply making R_1 proportional to R_2,

$$R_1 = g_1 \frac{k_1 S_1^n + a_2 b_2 S_2^n}{1 + k_1 S_1^n + b_2 S_2^n} R_2 \tag{6}$$

$$R_2 = g_2 \frac{a_1 b_1 S_1^n + k_2 S_2^n}{1 + b_1 S_1^n + k_2 S_2^n} \tag{7}$$

We may remove the parameters g_i and k_i by rescaling $S_1^n \leftarrow S_1^n/k_1$, $S_2^n \leftarrow S_2^n/k_2$, $R_1 \leftarrow g_1 g_2 R_1$, and $R_2 \leftarrow g_2 R_2$, and redefining parameters $b_1 \leftarrow b_1 k_1$, $b_2 \leftarrow b_2 k_2$. After such rescaling the equations finally become:

$$S_1 = f_1 R_1 \tag{8}$$

$$S_2 = f_2 R_2 \tag{9}$$

$$R_1 = \frac{S_1^n + a_2 b_2 S_2^n}{1 + S_1^n + b_2 S_2^n} R_2 \tag{10}$$

$$R_2 = \frac{a_1 b_1 S_1^n + S_2^n}{1 + b_1 S_1^n + S_2^n} \tag{11}$$

Numerical methods for finding solutions

To find the solutions to Eqs. (8–11), we consider a system of differential equations whose equilibrium states are the solutions to those equations above. The differential equations we use are:

$$\frac{dS_1}{dt} = \frac{1}{\tau_S}\left(f_1 R_1 - S_1\right) \tag{12}$$

$$\frac{dS_2}{dt} = \frac{1}{\tau_S}\left(f_2 R_2 - S_2\right) \tag{13}$$

$$\frac{dR_1}{dt} = \frac{1}{\tau_R}\left(\frac{S_1^n + a_2 b_2 S_2^n}{1 + S_1^n + b_2 S_2^n} R_2 - R_1\right) \tag{14}$$

$$\frac{dR_2}{dt} = \frac{1}{\tau_R}\left(\frac{a_1 b_1 S_1^n + S_2^n}{1 + b_1 S_1^n + S_2^n} - R_2\right) \tag{15}$$

where the timescales are set to $\tau_S = \tau_R = 1$ for simplicity. For each set of parameter values, we integrate these equations using the SciPy function solve_IVP() for 500 time units, starting from random initial values. This should bring the variables sufficiently close to a local equilibrium. We then refine the result using SciPy's root-finding function scipy.optimize.root(), with the previous result as the initial guess. Alongside this, we calculate the Jacobian matrix of our system of equations to verify that the equilibrium that we have found is stable. In order to find all potential solutions for a given set of parameters, we repeat this process 100 times with different random initial values and eliminate any duplicate solutions. To generate Figs. 2, 3, 4, 5 and 6 in the main text, we scan over the parameter space and apply the above procedure at every grid point in the parameter space. For the stochastic simulations in Fig. 9, we use $\tau_S = 1$ and $\tau_R = 0.1$; a random Gaussian noise is added to each equation with an amplitude $\sigma = 20$. The stochastic differential equations are integrated using the Euler–Maruyama method with a time step of $\Delta t = 0.0001$.

Analytic results at $n \to \infty$

In the limit $n \to \infty$, the solutions to Eq. (2) can be found using the following arguments:

(a) If both R_1 and R_2 are small, such that $f_1 R_1 < 1$ and $f_2 R_2 < 1$, then the right-hand side (RHS) would lead to $R_1, R_2 \to 0$. Indeed, $R_1 = R_2 = 0$ is always a solution.
(b) If $f_2 R_2 > 1$ and $f_2 R_2 > f_1 R_1$, then the RHS gives $R_2 = 1$ and $R_1 = a_2$. To be consistent, we need $f_2 > 1$ and $f_2 > a_2 f_1$, which corresponds to Regions II and III in Fig. 7.
(c) If $f_1 R_1 > f_2 R_2 > 1$, then the RHS gives $R_1 = R_2 = 1$. To be consistent, we need $f_1 > f_2 > 1$, which corresponds to Region III and part of Region IV in Fig. 7.
(d) If $f_1 R_1 > 1 > f_2 R_2$, then the result depends on b_1. For $b_1 > 0$, the RHS gives $R_1 = R_2 = 1$ as in (c), which corresponds to the $f_1 > 1 > f_2$ part of Region IV in Fig. 7. But for $b_1 = 0$, the RHS gives $R_1 = R_2 = 0$, which means this part is merged into Region I.

Taken together, the above arguments imply that:

(i) In Region I, the only solution is $(R_1, R_2) = (0, 0)$.
(ii) In Region II, both solutions (0, 0) and $(a_2, 1)$ are possible.
(iii) In Region III, three solutions are possible, (0, 0), $(a_2, 1)$, and (1, 1).
(iv) In Region IV, two solutions are possible, (0, 0) and (1, 1).

These different regions are shown in Fig. 7.

In some regions of interest, approximate solutions can be obtained to understand the behavior of the system. In the case where f_1 is small (left part of Region II), we can approximate that $S_1 \approx 0$. This allows us to ignore the effect of S_1 and simplify the equations to:

$$S_2 = f_2 R_2 \tag{16}$$

$$R_2 = \frac{S_2}{1 + S_2} \tag{17}$$

$$R_1 = \frac{a_2 b_2 S_2}{1 + b_2 S_2} R_2 \tag{18}$$

In this region, the R_1 response is completely controlled by the crosstalk coming from the S_2-R_2 feedback loop, which is the "jump-start" scenario. The activation level of R_1 is controlled by the parameter a_2, while its dependence on b_2 is weak as long as the feedback f_2 is strong enough to highly express S_2 (i.e., $f_2 > 1/b_2$).

Similarly, when f_2 is small (lower part of Region IV), we can ignore S_2 and simplify the equations to:

$$S_1 = f_1 R_1 \tag{19}$$

$$R_1 = \frac{S_1}{1 + S_1} R_2 \tag{20}$$

$$R_2 = \frac{a_1 b_1 S_1}{1 + b_1 S_1} \tag{21}$$

In this case, when a_1 and b_1 are not too small, there is a feedback loop S_1-R_2-R_1 that can activate both responses R_1 and R_2 to a level controlled by a_1, which is the "push-start" scenario. For $a_1 = 1$, both responses can be fully activated as long as the feedback f_1 is strong enough ($f_1 > 1/b_1$). In other words, the responses can be turned on by tuning the parameter b_1 above a threshold $\sim 1/f_1$. Note that if we eliminate R_2 from Eqs. (20, 21), then R_1 as a function of S_1 is more nonlinear than a Hill's function with $n = 1$.

Data availability

All data generated or analysed during this study are included in this published article.

Received: 24 May 2023; Accepted: 31 October 2023
Published online: 06 November 2023

References

1. Papenfort, K. & Bassler, B. L. Quorum sensing signal-response systems in gram-negative bacteria. *Nat. Rev. Microbiol.* **14**, 576–588. https://doi.org/10.1038/nrmicro.2016.89 (2016).
2. Mukherjee, S. & Bassler, B. L. Bacterial quorum sensing in complex and dynamically changing environments. *Nat. Rev. Microbiol.* **17**, 371–382. https://doi.org/10.1038/s41579-019-0186-5 (2019).
3. Aframian, N. & Eldar, A. A bacterial tower of babel: Quorum-sensing signaling diversity and its evolution. *Annu. Rev. Microbiol.* **74**, 587–606. https://doi.org/10.1146/annurev-micro-012220-063740 (2020).
4. Hawver, L. A., Jung, S. A. & Ng, W. L. Specificity and complexity in bacterial quorum-sensing systems. *FEMS Microbiol. Rev.* **40**, 738–752. https://doi.org/10.1093/femsre/fuw014 (2016).
5. Waters, C. M. & Bassler, B. L. Quorum sensing: Cell-to-cell communication in bacteria. *Annu. Rev. Cell Dev. Biol.* **21**, 319–346. https://doi.org/10.1146/annurev.cellbio.21.012704.131001 (2005).
6. Gooding, J. R., May, A. L., Hilliard, K. R. & Campagna, S. R. Establishing a quantitative definition of quorum sensing provides insight into the information content of the autoinducer signals in Vibrio harveyi and Escherichia coli. *Biochemistry* **49**, 5621–5623. https://doi.org/10.1021/bi1001163 (2010).
7. Anetzberger, C. *et al.* Autoinducers act as biological timers in Vibrio harveyi. *PLoS ONE* **7**, 1–12. https://doi.org/10.1371/journal.pone.0048310 (2012).
8. Cornforth, D. M. *et al.* Combinatorial quorum sensing allows bacteria to resolve their social and physical environment. *Proc. Natl. Acad. Sci.* **111**, 4280–4284. https://doi.org/10.1073/pnas.1319175111 (2014).
9. Even-Tov, E. *et al.* Social evolution selects for redundancy in bacterial quorum sensing. *PLoS Biol.* **14**, e1002386. https://doi.org/10.1371/journal.pbio.1002386 (2016).
10. Li, P., Elowitz, M. B., Klein, A. & Treutlein, B. Communication codes in developmental signaling pathways. *Development* **146**. https://doi.org/10.1242/dev.170977 (2019).
11. Wellington, S. & Greenberg, E. P. Quorum sensing signal selectivity and the potential for interspecies cross talk. *mBio* **10**, 1–14. https://doi.org/10.1128/mBio.00146-19 (2019).
12. Wu, F., Menn, D. J. & Wang, X. Quorum-sensing crosstalk-driven synthetic circuits: From unimodality to trimodality. *Chem. Biol.* **21**, 1629–1638. https://doi.org/10.1016/j.chembiol.2014.10.008 (2014).

13. Henke, J. M. & Bassler, B. L. Three parallel quorum-sensing systems regulate gene expression in Vibrio harveyi. *J. Bacteriol.* **186**, 6902–6914. https://doi.org/10.1128/JB.186.20.6902-6914.2004 (2004).
14. Kirby, D., Rothschild, J., Smart, M. & Zilman, A. Pleiotropy enables specific and accurate signaling in the presence of ligand cross talk. *Phys. Rev. E* **103**, 042401. https://doi.org/10.1103/PhysRevE.103.042401 (2021).
15. Laub, M. T. & Goulian, M. Specificity in two-component signal transduction pathways. *Annu. Rev. Genet.* **41**, 121–145. https://doi.org/10.1146/annurev.genet.41.042007.170548 (2007).
16. Carballo-Pacheco, M. *et al.* Receptor crosstalk improves concentration sensing of multiple ligands. *Phys. Rev. E* **99**, 22423. https://doi.org/10.1103/PhysRevE.99.022423 (2019).
17. Ostovar, G., Naughton, K. & Boedicker, J. Computation in bacterial communities. *Phys. Biol.* **17**, 061002. https://doi.org/10.1088/1478-3975/abb257 (2020).
18. Colton, D. M., Stabb, E. V. & Hagen, S. J. Modeling analysis of signal sensitivity and specificity by Vibrio fischeri LuxR variants. *PLoS ONE* **10**, 1–21. https://doi.org/10.1371/journal.pone.0126474 (2015).
19. Grant, P. K. *et al.* Orthogonal intercellular signaling for programmed spatial behavior. *Mol. Syst. Biol.* **12**, 1–13. https://doi.org/10.15252/msb.20156590 (2016).
20. Verma, S. & Miyashiro, T. Quorum sensing in the squid-vibrio symbiosis. *Int. J. Mol. Sci.* **14**, 16386–16401. https://doi.org/10.3390/ijms140816386 (2013).
21. Kimbrough, J. H. & Stabb, E. V. Substrate specificity and function of the pheromone receptor ainr in Vibrio fischeri es114. *J. Bacteriol.* **195**, 5223–5232. https://doi.org/10.1128/JB.00913-13 (2013).
22. Miyashiro, T. & Ruby, E. G. Shedding light on bioluminescence regulation in Vibrio fischeri. *Mol. Microbiol.* **84**, 795–806. https://doi.org/10.1111/j.1365-2958.2012.08065.x (2012).
23. Schaefer, A., Hanzelka, B., Eberhard, A. & Greenberg, E. Quorum sensing in Vibrio fischeri: probing autoinducer-luxr interactions with autoinducer analogs. *J. Bacteriol.* **178**, 2897–901. https://doi.org/10.1128/jb.178.10.2897-2901.1996 (1996).
24. Mehta, P., Goyal, S., Long, T., Bassler, B. L. & Wingreen, N. S. Information processing and signal integration in bacterial quorum sensing. *Mol. Syst. Biol.* **5**, 325. https://doi.org/10.1038/msb.2009.79 (2009).
25. Perez, P. D., Weiss, J. T. & Hagen, S. J. Noise and crosstalk in two quorum-sensing inputs of Vibrio fischeri. *BMC Syst. Biol.* **5**, 153. https://doi.org/10.1186/1752-0509-5-153 (2011).
26. Kuttler, C. & Hense, B. A. Interplay of two quorum sensing regulation systems of Vibrio fischeri. *J. Theor. Biol.* **251**, 167–180. https://doi.org/10.1016/j.jtbi.2007.11.015 (2008).
27. Kuo, A., Callahan, S. M. & Dunlap, P. V. Modulation of luminescence operon expression by n-octanoyl-l-homoserine lactone in ainS mutants of Vibrio fischeri. *J. Bacteriol.* **178**, 971–976. https://doi.org/10.1128/jb.178.4.971-976.1996 (1996).
28. Lupp, C., Urbanowski, M., Greenberg, E. P. & Ruby, E. G. The Vibrio fischeri quorum-sensing systems ain and lux sequentially induce luminescence gene expression and are important for persistence in the squid host. *Mol. Microbiol.* **50**, 319–331. https://doi.org/10.1046/j.1365-2958.2003.t01-1-03585.x (2003).
29. Bose, J. L. *et al.* Contribution of rapid evolution of the luxR-luxI intergenic region to the diverse bioluminescence outputs of Vibrio fischeri strains isolated from different environments. *Appl. Environ. Microbiol.* **77**, 2445–2457. https://doi.org/10.1128/AEM.02643-10 (2011).
30. Anetzberger, C., Pirch, T. & Jung, K. Heterogeneity in quorum sensing-regulated bioluminescence of Vibrio harveyi. *Mol. Microbiol.* **73**, 267–277. https://doi.org/10.1111/j.1365-2958.2009.06768.x (2009).
31. Haseltine, E. L. & Arnold, F. H. Implications of rewiring bacterial quorum sensing. *Appl. Environ. Microbiol.* **74**, 437–445. https://doi.org/10.1128/AEM.01688-07 (2008).
32. Williams, J. W., Cui, X., Levchenko, A. & Stevens, A. M. Robust and sensitive control of a quorum-sensing circuit by two interlocked feedback loops. *Mol. Syst. Biol.* **4**, 234. https://doi.org/10.1038/msb.2008.70 (2008).
33. Underhill, S. *et al.* Intracellular signaling by the *comRS* system in *Streptococcus mutans* genetic competence. *mSphere* **3**, e00444–18. https://doi.org/10.1128/mSphere.00444-18 (2018).
34. Striednig, B. & Hilbi, H. Bacterial quorum sensing and phenotypic heterogeneity: How the collective shapes the individual. *Trends Microbiol.* **30**, 379–389. https://doi.org/10.1016/j.tim.2021.09.001 (2022).
35. Bettenworth, V. *et al.* Phenotypic heterogeneity in bacterial quorum sensing systems. *J. Mol. Biol.* **431**, 4530–4546. https://doi.org/10.1016/j.jmb.2019.04.036 (2019).

Acknowledgements

Funding support from National Science Foundation award MCB 1715981 to S.J.H. is acknowledged.

Author contributions

S.J.H. and B.K.X. conceived the study, J.G.S. and H.A. conducted the study and analysed the results. J.G.S., S.J.H., and B.K.X. wrote the manuscript.

Competing interests

The authors declare no competing interests.

Additional information

Supplementary Information The online version contains supplementary material available at https://doi.org/10.1038/s41598-023-46399-z.

Correspondence and requests for materials should be addressed to B.X.

Reprints and permissions information is available at www.nature.com/reprints.

Publisher's note Springer Nature remains neutral with regard to jurisdictional claims in published maps and institutional affiliations.

Open Access This article is licensed under a Creative Commons Attribution 4.0 International License, which permits use, sharing, adaptation, distribution and reproduction in any medium or format, as long as you give appropriate credit to the original author(s) and the source, provide a link to the Creative Commons licence, and indicate if changes were made. The images or other third party material in this article are included in the article's Creative Commons licence, unless indicated otherwise in a credit line to the material. If material is not included in the article's Creative Commons licence and your intended use is not permitted by statutory regulation or exceeds the permitted use, you will need to obtain permission directly from the copyright holder. To view a copy of this licence, visit http://creativecommons.org/licenses/by/4.0/.

© The Author(s) 2023